

# Flexible Piezoelectric ZnO–Paper Nanocomposite Strain Sensor

Hemtej Gullapalli, Venkata S. M. Vemuru, Ashavani Kumar, Andres Botello-Mendez, Robert Vajtai, Mauricio Terrones, Satish Nagarajaiah, and Pulickel M. Ajayan\*

*The fabrication of a mechanically flexible, piezoelectric nanocomposite material for strain sensing applications is reported. Nanocomposite material consisting of zinc oxide (ZnO) nanostructures embedded in a stable matrix of paper (cellulose fibers) is prepared by a solvothermal method. The applicability of this material as a strain sensor is demonstrated by studying its real-time current response under both static and dynamic mechanical loading. The material presented highlights a novel approach to introduce flexibility into strain sensors by embedding crystalline piezoelectric material in a flexible cellulose-based secondary matrix.*

## Keywords:

- cellulose fibers
- strain sensors
- nanocomposites
- piezoelectrics
- zinc oxide

## 1. Introduction

Critical infrastructures, including highways, buildings, bridges, aircraft, ships, and pipelines, form the lifeline of economic and industrial hubs and are sometimes subjected to

severe loading conditions due to extreme events such as earthquakes, hurricanes, and other natural disasters during their lifetime. To prevent catastrophic failures and subsequent loss of life, it is essential to continuously monitor the state of the structure and identify any initiation of damage in real time by using structural health monitoring (SHM) techniques, in particular strain sensing. SHM provides an autonomous way of tracking changes in the system in real time using a combination of instrumentation systems and analytical methods.<sup>[1,2]</sup> Instrumentation systems consist primarily of transducers to measure physical quantities, such as strain, displacement, and acceleration, which can give insight into the behavior of structures. Among the quantities of interest for SHM, strain is a local and direct measure of the state of the structure and is thus widely used as a reliable indicator of the damage induced in the structure. Hence, strain sensors are used extensively in SHM applications.

Strain gauges or transducers can be broadly classified into optical sensors, resistance-based sensors, and piezoelectric sensors. Among them, resistance-based sensors form the major portion of commercially available foil strain-gauge sensors.<sup>[3]</sup> Recent research and development of resistance sensors based on nanostructures<sup>[4,5]</sup> and their composites<sup>[6–10]</sup> has accelerated since the discovery of materials such as carbon nanotubes. Carbon-nanofilm strain sensors have been shown to provide multidirectional and multipoint strain sensing.<sup>[4]</sup> Nanomaterial-based sensor technology is yet to find commercial applications and is still in the development stage. Furthermore, power requirements are a major limitation and hinder large-scale

[\*] Prof. P. M. Ajayan, H. Gullapalli, Dr. A. Kumar, Dr. R. Vajtai, Prof. S. Nagarajaiah  
Department of Mechanical Engineering and Material Science  
Rice University  
6100 Main St., Houston, TX 77005 (USA)  
E-mail: ajayan@rice.edu

V. S. M. Vemuru, Prof. S. Nagarajaiah  
Department of Civil and Environmental Engineering  
Rice University  
6100 Main St., Houston, TX 77005 (USA)

A. Botello-Mendez  
Laboratory for Nanoscience and Nanotechnology Research (LINAN)  
and Advanced Materials Department, IPICT  
Camino a la Presa San José 2055, Col. Lomas 4<sup>a</sup> sección,  
San Luis Potosí 78216 (México)

Prof. M. Terrones  
Department of Physics and Mathematics  
Division of Science, Arts, and Technology  
Universidad Iberoamericana  
Avenida Prolongación Paseo de la Reforma 880, Santa Fé 012100,  
DF (México)

Supporting Information is available on the WWW under <http://www.small-journal.com> or from the author.

DOI: 10.1002/sml.201000254

deployment of instrumentation for SHM, hence strain transducers with low power requirements are highly desirable.

Piezoelectric materials have the ability to convert mechanical energy into electrical energy and have long been used for strain sensing. Among other types of sensors, piezoelectric sensors have the lowest power requirements<sup>[3]</sup> and the charge output from piezoelectric sensors lies within the range of measurement capabilities of commercially available analog/digital sensors. Lead zirconate titanate (PZT) is a common piezoelectric material that is commercially used for piezoelectric actuators and sensors. Other applications, for example energy harvesting using such piezoelectric materials, have also been studied.<sup>[11]</sup> Recently, Wang and co-workers fabricated a ZnO piezoelectric fine-wire-based strain sensor, wherein ZnO fine wires were laterally bonded with a polystyrene substrate and used to measure strain.<sup>[12]</sup>

Pure crystalline forms of piezoelectric materials such as PZT or ZnO, when used as strain sensors, are usually bonded on the surface or embedded inside the host structure for strain measurement and have limitations to measure strain at discrete points and in a fixed direction. Pure piezoelectric materials are mostly brittle ceramics that are not amenable to flexible applications and are very weak in tension.<sup>[13]</sup> Furthermore, it is observed in the literature that combined mechanical and electrical loading might lead to premature cracking in piezoelectric materials, which markedly affects their behavior.<sup>[14]</sup> Certain studies have demonstrated the fabrication of flexible piezoelectric sensors or actuators but require special techniques, thus making it uneconomical for large-scale synthesis.<sup>[15,16]</sup> Although other materials were also used for flexible strain sensors, they lack the unique properties of piezoelectric materials or involve complicated fabrication techniques. Therefore, there is a need to develop simple, scalable, inexpensive, and mechanically flexible sensors that can be embedded into a material or form fitted easily onto an existing structure and used for multidirectional sensing over a practically viable sensing region. Avoiding lead-based products is also eco-friendly and essential for use in next-generation clean technology.

Herein, we demonstrate a low-temperature solvothermal method for the synthesis of a nanocomposite material consisting of ZnO nanostructures embedded in a paper (cellulose) matrix. Since ZnO is a well-known material for piezoelectric applications, it has a wide range of uses such as strain sensing, acoustic sensing,<sup>[17]</sup> and energy harvesting.<sup>[18]</sup> The presence of the paper matrix makes the composite material very flexible. We demonstrate strain sensing under both static and dynamic loading using this nanocomposite material. Its performance is evaluated and compared to that of the commercially available strain gauges.

## 2. Results and Discussion

Crystal structure and surface morphology characterizations of ZnO–cellulose composite paper are shown in Figure 1. Figure 1a presents the X-ray diffraction (XRD) spectra of the ZnO-coated paper showing various Bragg reflections corresponding to the ZnO wurtzite structure. The insets of Figure 1a are optical images showing the flexibility of the composite paper. The flexibility of the paper was fairly retained even after coating it with ZnO. Figure 1b–d shows low- and high-magnification scanning electron microscopy (SEM) images of a cellulose paper before and after coating with ZnO. The initial paper is highly porous and composed of micrometer-sized fibers that are randomly oriented. The fibers are quite smooth before coating with ZnO, with a diameter in the range of  $\approx 5$  to  $15\ \mu\text{m}$  (Figure 1b). These fibers become very rough after deposition of ZnO, as seen in Figure 1c. The higher-magnification image shows the nanorods grown from the surface with typical diameters in the range of 40–100 nm and lengths between 500 and 1000 nm.

The ZnO rods grown on the cellulose paper were further characterized by transmission electron microscopy (TEM). The ZnO rods were dispersed in ethanol and dropped onto a carbon-coated copper grid. The rods are uniform and discrete with a diameter of  $\approx 20$  nm (Figure 2). The high-resolution TEM image (Figure 2c) reveals the uniform crystalline nature of the rods, with the fast Fourier transform (FFT) depicting the (002) plane of the ZnO crystal. These rods grow perpendicular to the cellulose fibers.

The growth mechanism of the nanocomposite can be explained as follows. When zinc acetate solution is added and

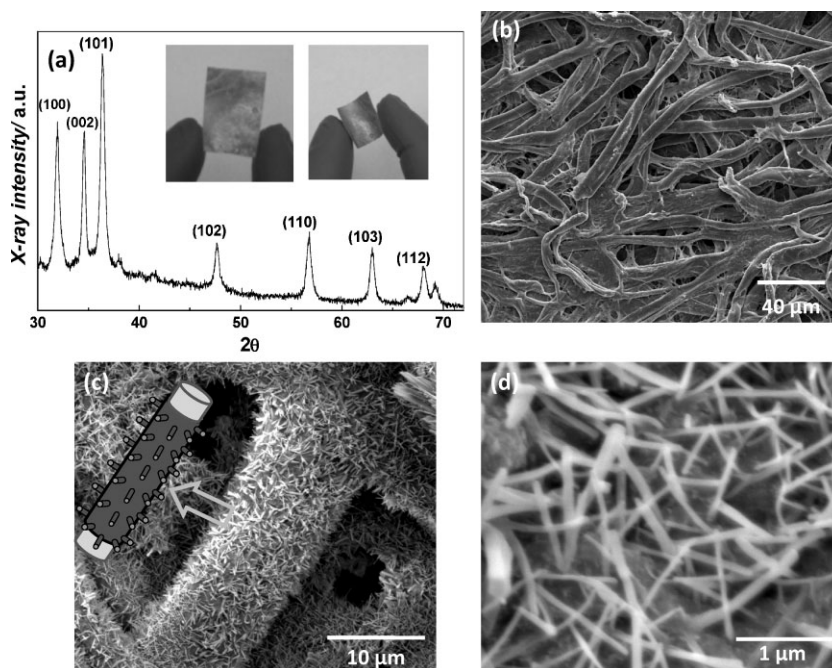


**Figure 1.** a) XRD spectra of ZnO–paper composite confirming the crystalline structure. The first three peaks are predominant for cellulose fibers. b) SEM image showing the morphology of a commercial paper before it is coated with ZnO. c) SEM image showing the morphology of the ZnO–paper composite. Inset: schematic depiction of the structure; a thin film of ZnO is formed around the paper fiber and nanorods grow axially outwards. d) High-magnification SEM image of the composite showing the crystalline ZnO nanorods.

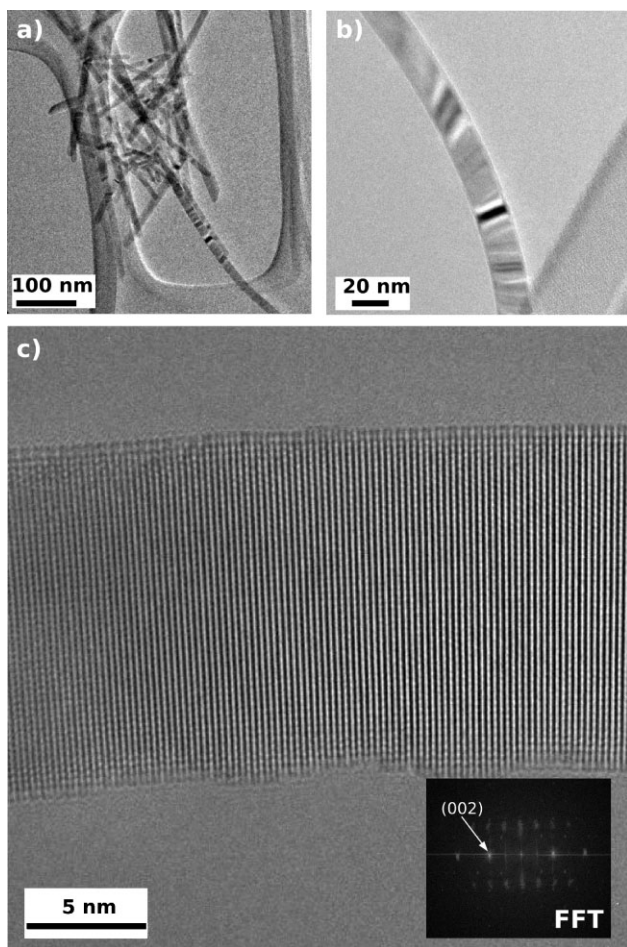


**Figure 2.** a,b) TEM images of ZnO nanorods taken from the composite paper. c) High-resolution TEM image of a single nanorod showing its crystalline nature; inset: FFT spectrum identifying the lattice orientation as (002).

dried on the paper, the fibers are coated evenly with zinc acetate nanoparticles. Later, when sodium hydroxide solution is added, hydrolysis results in the formation of ZnO nanoparticles. Due to the continuous deposition of these ZnO nanoparticles, their concentration increases to form a quasi-continuous film in which the nanoparticles are concentrated in certain areas. These concentrated areas act as nucleating sites for the growth of crystalline nanostructures. By maintaining an optimum temperature, crystal growth is favored thus resulting in the growth of a continuous film followed by nanorods at these sites (shown in Figure 1d).

The experimental configuration for strain-sensor measurements under static loading is shown schematically in Figure 3a. The current–voltage ( $I$ – $V$ ) characteristic curves of the nanocomposite sensor at different strains indicate a shift with increasing tension (Figure 3b). Figure 3c shows the current response from the nanocomposite sensor and the strain reading from the commercial strain gauge for a stepped tensile loading. The nanocomposite sensor was tested under cyclic loading conditions in both compression and tension, as shown in Figure 3d. The loading was carried out at a very low rate, and hence no dynamic effects of the brass beam are

observed in the response. A voltage bias of 0.1 V was applied for the results presented in Figure 3. The behavior of the nanocomposite sensor as it is subjected to constant load is tested by applying a tensile load to the specimen in increments as shown in Figure 3c. It is evident from the electrical response that the nanocomposite sensor demonstrates a stable response both when the load is increasing as well as when it remains constant at a given level. The electrical response from the nanocomposite sensor is found to be in good agreement with the strain measured by a foil strain gauge for static loading. The nanocomposite sensor behaves in a similar manner in both compression and tension, as demonstrated by the response of the sensor to cyclic loading (Figure 3d), and it is evident that even after repeated cycles no drift is observed in the response.

The strain-dependent response in the paper is due to the piezoelectric property of the ZnO coated on it and can be explained as follows. The strain transferred from the beam creates two types of stresses on the ZnO-coated paper: a) as the cellulose fibers are deformed, the nanorods on their surfaces are rubbed against each other, which causes them to deflect and generates a potential difference (or piezoelectric potential) along the nanowire diameter; and b) since the fibers are coated with a ZnO thin film, there is a strain due to the deformation of the fibers. The ion displacement due to this strain creates a difference of potential along the thin film. The potential difference that drives the current from one electrode to the other is in the ZnO thin film and the difference of potential within individual nanorods barely contributes.

The signal-to-noise ratio is also very high for the response observed. The gauge factor (GF) of the nanocomposite sensor can be calculated using the modified formula<sup>[19]</sup> as follows:

$$GF = \frac{\Delta R/R}{\varepsilon} = \frac{\Delta i/i_f}{\varepsilon} = \frac{(i_0 - i_f)}{i_f \times \varepsilon} \quad (1)$$

where  $\varepsilon$  is the strain applied to the sensor,  $i_0$  is the initial current at zero strain, and  $i_f$  is the final current at  $\varepsilon$  strain. From the observed results the GF of the nanocomposite sensor was found to be  $\approx 21.12$ , which is comparable to the generally recorded values for commercial strain gauges.

The response of the sensor was also studied for dynamic loading as shown in Figure 4. Figure 4a depicts the experimental setup used for such dynamic testing. The actuator was excited at various frequencies keeping the excitation amplitude constant, and the response of the composite sensor was measured without the application of any input voltage. The measured response from the sensor at frequencies of 0.1, 1, 2, and 4 Hz is presented in Figure 4b–d and f, respectively. The excitation was applied in repeated sets of cycles of sinusoidal excitation. The frequency of the response corresponds well with the frequency of excitation; a consistent behavior in the response of the sensor is observed for different frequencies. Figure 4e shows a closer view of the response and illustrates the reproducibility under cyclic loading. Also, no drift was observed in the response at

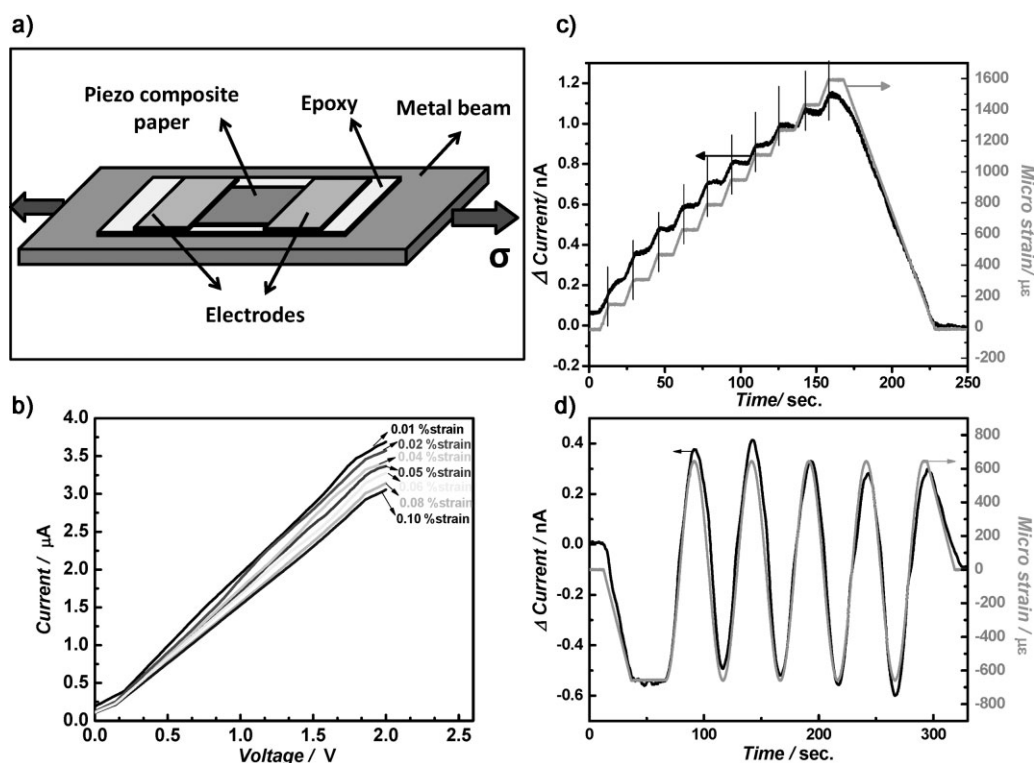


**Figure 3.** a) Schematic depicting the experimental setup for strain measurement under static loading. b)  $I$ - $V$  characteristic of the composite sensor as a function of strain; a shift is observed in the  $I$ - $V$  curves with a change in applied strain. c) Response of the composite sensor to tensile loading, which was increased in steps (of 44.48 kN) with intermittent constant-loading intervals, compared to strain measured by a commercial strain gauge. d) Response of the composite sensor to cyclic loading in which a load is cycled equally from compression to tension ( $-26.69$  to  $+26.69$  kN), compared to strain measured by a commercial strain gauge.

the end of each cycle of excitation. The amplitude of the response of the sensor is observed to increase with increasing frequency, because the amplitude of vibration of the beam increases with increasing input frequency. The first resonant frequency of the beam was observed to be at a value higher than 4 Hz. The nanocomposite sensor showed good strain sensitivity for deformations in both tension and compression corresponding to the positive and negative peaks of the response. Due to the piezoelectric nature of the nanocomposite, it can be operated without any source power as demonstrated in this test, thus opening the possibility of self-powered sensors.

### 3. Conclusions

In summary, we have presented a technique to embed piezoelectric ZnO into commercial paper, by using a simple and scalable synthesis method. By making a continuous coating of ZnO nanostructures on a flexible matrix such as paper, flexibility can be introduced without loss of its piezoelectric properties. The composite sensor can be molded as sensor devices, and shows characteristics of good sensitivity and linearity at different frequencies. The mechanically robust nature of the sensor also makes it amenable to field applications in SHM. We have demonstrated good strain sensitivity for both static and dynamic loading with very low

power input. The nanocomposite material has potential applications as a flexible, robust, self-powered sensor in structural applications.

## 4. Experimental Section

**Synthesis of ZnO-embedded paper:** For preparing the ZnO paper, a sol-gel synthesis method was employed. Sol A was prepared by dissolving zinc acetate dihydrate solution (0.1 M) in ethanol (200 proof, 50 mL) at 60 °C. Sol B was prepared by dissolving NaOH (1 M) in ethanol (200 proof, 50 mL). A plain printing paper (70 mm in diameter, 0.47 mm thick) was placed in a petri dish. It was then soaked dropwise with sol A, dried at 100 °C in an oven, soaked with sol B, and dried again. Several repetitions of the above procedure with occasional washing with distilled water to remove any by-products resulted in uniform coating of ZnO crystals over individual fibers of the cellulose paper. The typical composition of ZnO in the resultant composite was 40 wt%.

For electrical contacts, a thin layer of gold was deposited on the surface of the resulting ZnO-paper with a plasma sputtering system. The devices were poled initially by applying a dc voltage of 20 V for 30 s and then shorting the terminals for a few minutes to drain out any residual charge. Morphological and elemental

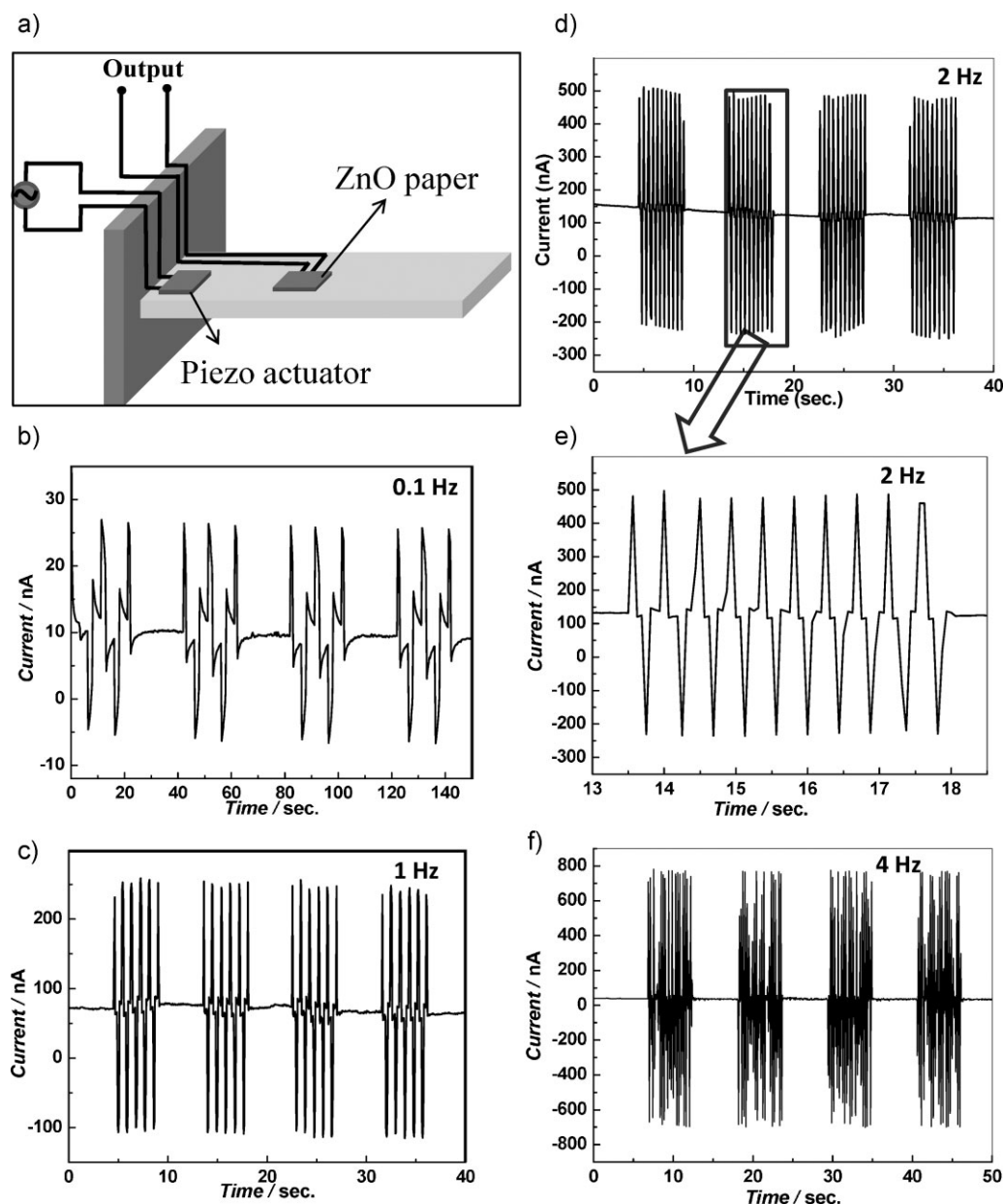


**Figure 4.** a) Schematic depicting the experimental setup for strain measurement under dynamic loading. b–f) Dynamic response of the composite sensor on exciting the beam with frequencies b) 0.1, c) 1, d,e) 2, and f) 4 Hz. The frequency of the dynamic response matches closely the excitation frequency.

analysis of the composite material was carried out using a scanning electron microscope (FEI Quanta 400) operated at 20 kV and equipped with an energy-dispersive X-ray spectrometry (EDS) detector. The crystalline nature of the products was determined using an X-ray diffractometer (Rigaku D/Max Ultima II) operated at 40 kV and with  $\text{CuK}\alpha$  radiation.

**Setup for strain sensing:** For the fabrication of a typical composite sensor specimen, a piece of the ZnO paper ( $2 \times 0.5 \text{ cm}^2$ ) was coated with two gold electrodes on the surface, separated by a distance of  $\approx 0.3 \text{ mm}$ . For static strain measurements, the specimen was attached to a brass beam (cross sectional area  $3.17 \times 0.635 \text{ cm}^2$  with Young's modulus 166 GPa)

using a thin coat of insulating epoxy. A conventional, commercial-grade foil strain gauge (Vishay Intertechnology Inc., PA, with a GF of 2.1) was also attached to the beam for comparison. Both the strain gauge and the composite sensor were oriented along the length of the beam. The brass beam was mounted in a MTS hydraulic testing machine and an axial load was applied along its length.

For dynamical testing and measurement, the piezo-paper was attached with superglue to an aluminum strip of cross section  $50 \times 0.7 \text{ mm}^2$  and having a Young's modulus of 69 GPa, as shown in Figure 4a. Another commercial metallic foil strain gauge was attached on the opposite side of the aluminum specimen for strain measurement comparisons. A piezo actuator (from Mide

Technology Corporation, MA) was attached to the aluminum specimen to excite the beam at different frequencies for a fixed duration. The piezo actuator was operated using a dSPACE Data Acquisition unit in conjunction with a power amplifier. The beam was excited with the external piezo-patch for a range of frequencies.

The performance of the composite sensor to applied static load was evaluated by measuring its output current using a Keithley Series 2400 Digital Source Meter (with a sensitivity of 10 pA and a sampling rate of 100 samples  $s^{-1}$ ) and compared with the strain measured using a commercial foil strain gauge. The measurement for the composite sensor was carried out using insulated/sheathed cables taking care to minimize the influence of surrounding noise.

## Acknowledgements

This work was supported in part by CONACYT-México grants: 56787 (Laboratory for Nanoscience and Nanotechnology Research-LINAN), 45772 (M.T.), 41464 and 58899-Inter-American Collaboration (M.T.), and a PhD Scholarship (A.B.M.). V.S.M.V. and S.N. acknowledge support provided by the Air Force Office of Scientific Research. P.M.A. acknowledges Rice University faculty startup funds.

- 
- [1] C. R. Farrar, S. W. Doebling, A. D. Nix, *Philos. Trans. R. Soc. London A* **2001**, *359*, 131–149.  
 [2] S. W. Doebling, C. R. Farrar, M. B. Prime, *Shock Vib. Dig.* **1998**, *30*, 91–105.

- [3] G. Park, T. Rosing, M. D. Todd, C. R. Farrar, W. Hodgkiss, *ASCE J. Infrastruct. Syst.* **2008**, *14*, 64–79.  
 [4] P. Dharap, Z. Li, S. Nagarajaiah, E. V. Barrera, *Nanotechnology* **2004**, *15*, 379–382.  
 [5] Z. Li, P. Dharap, S. Nagarajaiah, E. V. Barrera, J. D. Kim, *Adv. Mater.* **2004**, *16*, 640–643.  
 [6] I. Kang, M. J. Schulz, J. H. Kim, V. Shanov, D. Shi, *Smart Mater. Struct.* **2006**, *15*, 737–748.  
 [7] K. J. Loh, J. P. Lynch, B. S. Shim, *J. Intell. Mater. Syst. Struct.* **2008**, *19*, 747–764.  
 [8] W. Zhang, J. Suhr, N. Koratkar, J. Nanosci, *Nanotechnology* **2006**, *6*, 960–964.  
 [9] M. K. Tiwari, A. L. Yarin, C. M. Megaridis, *J. Appl. Phys.* **2008**, *103*, 044305–10.  
 [10] O. Aldraihem, W. N. Akl, A. M. Baz, *Sens. Actuators A* **2000**, *149*, 233–240.  
 [11] H. A. Sodano, G. Park, D. J. Inman, *Strain* **2004**, *40*, 49–58.  
 [12] J. Zhou, P. Fei, Y. Gu, W. Mai, Y. Gao, R. Yang, G. Bao, Z. L. Wang, *Nano Lett.* **2008**, *8*, 3973–3977.  
 [13] L. Fixter, C. Williamson, State of the Art Review—Structural Health Monitoring, Smart Materials, Surfaces, and Structures Network (Smart.Mat) Report, 2006.  
 [14] S. Kumar, R. N. Singh, *Acta Mater.* **1996**, *44*, 173–200.  
 [15] F. Mohammed, A. Khan, R. B. Cass, *Mater. Res. Soc. Symp. Proc.* **2003**, p. 736.  
 [16] C. S. Lee, J. Joo, S. Han, S. K. Koh, *Appl. Phys. Lett.* **2004**, *85*, 1841–1843.  
 [17] M. Royer, J. O. Holmen, M. A. Wurm, O. S. Aadland, M. Glenn, *Sens. Actuators* **1983**, *4*, 357–362.  
 [18] Z. L. Wang, J. Song, *Science* **2006**, *312*, 242–246.  
 [19] H. G. Harris, G. Sabnis, *Structural Modeling and Experimental Techniques*, 2nd ed. CRC, Boca Raton **1999**.

Received: February 17, 2010  
 Revised: March 22, 2010  
 Published online: July 7, 2010